



Solid Electron Acceptor Effect on Biocatalyst Activity in Treating Azo dye Based Wastewater

Journal:	<i>RSC Advances</i>
Manuscript ID	RA-ART-08-2015-015648.R1
Article Type:	Paper
Date Submitted by the Author:	06-Oct-2015
Complete List of Authors:	S, Sreelatha; CSIR-Indian Institute of chemical Technology, Gokuladoss, Velvizhi; Indian Institute of Chemical Technology, Bioengineering and Environmental Centre C, Nagendranataha Reddy; CSIR-Indian Institute of chemical Technology, Bio-engineering and Environmental sciences (BEES); Indian Institute of Chemical Technology, Bioengineering and Environmental Centre Annie Modestra, Jampala; Indian Institute of Chemical Technology, Bioengineering and Environmental Centre Venkata Mohan, S; Indian Institute of Chemical Technology, Bioengineering and Environmental Centre
Subject area & keyword:	Biofuels & biomass < Energy

34 1. Introduction

35 Azo compounds are characterized by its possession of one or more azo chemical moieties
36 (-N=N-) and their linkages in a chemical compound could be flanked by alkyl or aryl groups.
37 Presence of sulfo and azo groups in the dye structure, protects the dye molecule from attack
38 of oxygenases making them resistant for oxidative biodegradation.¹ Hence these compounds
39 are more difficult to degrade through conventional aerobic treatment process.¹⁻³ Azo dye
40 molecule requires sequential redox conditions to cleave the chromophore (anaerobic) into
41 corresponding aromatic amines and further degradation (aerobic) of toxic aromatics into
42 simpler compounds.⁴⁻⁶ The process of anaerobic degradation supports reductive breakdown
43 of dye molecule by cleaving the chromophore into corresponding colourless aromatic
44 amines.⁷ This breakdown is supported by the utilization of redox powers obtained by
45 oxidation of co-substrate in the surrounding microenvironment. Previous studies by Sreelatha
46 et al. (2015) evaluated the dye based wastewater treatment in anaerobic systems and achieved
47 considerable treatment efficiency.⁷ Although anaerobic treatment has the potential to treat azo
48 dyes to some extent, it cannot be used as standalone process and may be used in concurrence
49 with current technologies to achieve better treatment.

50 Bioelectrochemical systems (BES) are typically a type of Microbial fuel cell (MFC), a
51 promising technology for electricity production which can be advantageously combined with
52 applications in wastewater treatment.^{8,9} When the major attention is on treatment rather than
53 electricity production, BES can also be called as bioelectrochemical treatment systems
54 (BET).^{10,11} BET use electrodes as solid electron acceptor for bacteria respiration and exploit
55 microbial catabolic activities to generate electrons (e^-) and protons (H^+) by degrading organic
56 molecules. The microbial metabolism is linked via electron donating and accepting
57 conditions through the presence of artificially introduced electrodes (anode and cathode) that
58 induces the development of potential difference which acts as a net driving force for
59 bioelectrogenic activity and complex pollutant removal.^{12,13} BET has the potential to
60 overcome the above limitations by converting chemical energy to electrical energy through
61 cascade of redox reactions with simultaneous waste remediation.

62 BET performance is governed by various parameters that regulate the performance viz.,
63 physical, physico-chemical, chemical, biological, electrochemical, etc. One of the important
64 factors is the biological factor where the microbes/bacteria acts as biocatalyst that will
65 undergo diverse biochemical pathways and acquire various electron transfer mechanisms
66 influencing the electron transfer rate and bioelectricity generation.¹¹ Bacteria as biocatalyst

67 will discharge reducing equivalents upon substrate degradation and will aid in the
68 pollutant/wastewater degradation.

69 Besides, the important physical factor to be considered in BET operation is the presence of
70 electrode assembly functioning as anode and cathode respectively. The electrode assembly in
71 BET system acts as a solid electron acceptor and enables the bacterial respiration on its
72 surface. Anode respiring bacteria (ARB) will respire on the electrode surface enabling
73 electron transfer effectively towards dye/wastewater degradation. BET has the advantage of
74 coupling both electrochemical and anaerobic biological processes which triggers the redox
75 reactions for the degradation of complex pollutants with simultaneous power generation.⁹

76 Considering the specific functions of biological and physical factors of BET system, present
77 study is designed to evaluate the influence of bacteria as biocatalyst and electrode assembly
78 as solid electron acceptor for treatment of azo dye compounds. The experiment was evaluated
79 using three different experimental operations principally with BET system comprising of
80 both bacteria and electrode assembly in comparison to anaerobic treatment (AnT) and
81 abiotic-control comprising of electrode assembly without biocatalyst. The specific influence
82 of electrode assembly as a solid electron acceptor and the variation in biocatalyst behaviour
83 with respect to electrode assembly was evaluated using mixed consortia as biocatalyst and
84 non-catalyzed graphite electrodes as anode and cathode in BET system. All the three systems
85 were simultaneously operated to assess the relative performance in conjunction with
86 biocatalyst and solid electron acceptor during azo dye reduction.

87 **2. Materials and Methods**

88 **2.1 Biocatalyst**

89 An indigenous mixed anaerobic sludge acquired from effluent treatment plant (ETP-
90 Hyderabad) was used as biocatalyst for the experimentation. The inoculum, prior to
91 experimentation was washed twice with phosphate buffer saline and re-suspended in DSW
92 (COD: 3 g/l (without dye) overnight at ambient room temperature. The grown culture was
93 inoculated in to respective bioreactors by re-suspending through feed (VSS, 4660 mg/l) to
94 facilitate the initial adaptation and stabilization of microorganisms in the respective
95 bioreactors.

96 **2.2 Experimental Methodology**

97 The present study evaluates the influence of biocatalyst to decolorize azo dye based
98 wastewater using three different experimental setups viz., bioelectrochemical treatment

99 (BET; electrode assembly and biocatalyst), anaerobic treatment (AnT; without electrode
100 assembly and with biocatalyst) and Control (abiotic; with electrode assembly and without
101 biocatalyst). AnT configuration described in the present study is adopted from Sreelatha et
102 al. 2015. BET and control systems were operated using non-catalyzed graphite plates as
103 electrodes (5 x 5 cm; 10 mm thick; 70 cm² surface area) in a single chamber open air cathode
104 system. All the three reactors have a total/working volume of 0.50/0.45 l and were operated
105 in fed-batch mode for 15 cycles (720 h) with a hydraulic retention time (HRT) of 48 h for
106 each cycle. Comparison was made between BET and AnT to understand the influence of
107 electrode assembly in conjunction with biocatalyst during the operation.

108 C.I. Acid Black 10B [(4-amino-5-hydroxy-3-[(4-nitrophenyl) azo]-6-(phenyl azo)-2,7-
109 naphthalene disulfonic acid disodium salt (C₂₂H₁₄N₆O₉S₂Na₂), an azo dye belonging to acid
110 applications class was used as a test dye. The simulated dye wastewater (SDW) was prepared
111 by dissolving 50 mg/l of dye in designed synthetic wastewater [DSW (g/l): glucose-3.0,
112 NH₄Cl-0.5, KH₂PO₄-0.25, K₂HPO₄-0.25, MgCl₂-0.3, CoCl₂-0.025, FeCl₃- 0.025, ZnCl₂-
113 0.0115, NiSO₄-0.050, CuCl₂-0.0105, CaCl₂-0.005 and MnCl₂-0.015].¹⁰ Prior to feeding, the
114 pH of the SDW was adjusted to 7.1 ± 0.1 using 1N HCl/1 N NaOH.

115 **2.3 Enzymes activity**

116 **2.3.1 Azo Reductase activity**

117 Azo reductase activity was monitored to understand the reductive cleavage of azo bond in
118 dye molecule. Colorimetric method was employed to estimate the extracellular azo reductase
119 enzyme activity using co-substrate NADH¹⁴. To estimate enzyme activity, the reaction
120 mixture was prepared with 200 µl sample, 400 µl of potassium phosphate buffer and 200 µl
121 of C.I. Acid Black 10 B. The reaction was initiated by adding 200 µl of NADH (7 mg/ml)
122 and absorbance was monitored at 618 nm (Venkata Mohan et al., 2012, 2013a). The linear
123 decrease of absorption was used to calculate the azo reductase activity. One unit of azo
124 reductase can be defined as the amount of enzyme required to decolorize 1 µmol of dye per
125 minute. Well plate detection assay was performed by dissolving agar-agar (2%) in 100 ml
126 milli-q water along with 50 mg of azo dye followed by boiling at temperature (60° C). After
127 solidification, small and equal sized holes were made in the petri dish. First well was loaded
128 with 80 µl of partially purified protein sample and 20 µl of NADH (7 mg/ml). The second
129 well was loaded with crude protein extract (80 µl) followed by NADH. Well loaded only
130 with milli-q water and NADH served as control.¹⁴

131

132 2.3.2 Dehydrogenase activity

133 Dehydrogenase (DH) activity (substrate linked) of the anaerobic biocatalyst was estimated
134 using redox sensitive 2,3,5-triphenyltetrazolium chloride (TTC) based on the reduction to
135 insoluble formazan¹⁵. DH was analyzed by adding 5 ml of TTC (5 g/l) and 2 ml of glucose
136 solution (0.1 mol/l) to 5 ml of the bacterial culture and the resulting solution was stirred
137 continuously (20 min; 200 rpm) followed by incubation (37 °C; 12 h). Subsequently, 1 ml of
138 concentrated sulphuric acid was added to the reaction mixture to stop the deoxidation
139 followed by addition of 5 ml of toluene to extract triphenyl formazan (TF) formed in the
140 reaction mixture. The sample was agitated at 200 rpm (30 min). After keeping the reaction
141 mixture idle for 3 min, the sample was centrifuged at 4000 rpm (5 min) and the supernatant
142 was collected and the absorbance was measured at 492 nm using spectrophotometer (TF
143 forms a colored complex with toluene).

144 2.4 Analysis

145 The electrogenic performance of BET and abiotic-control systems having electrode assembly
146 was evaluated in terms of open circuit voltage (OCV) and current generation patterns. The
147 electrochemical behavior was assessed by performing polarization with the function of
148 current density against potential and power density measured at different resistances (30–0.05
149 kΩ). Anode potentials were also measured at variable external resistances to find the
150 sustainable power generation. Samples were analyzed for the change in dye and COD
151 concentrations and enzymes activities. Dye concentration was monitored colorimetrically at
152 λ_{max} 618 nm using UV-Vis spectrophotometer. Reactor performance was assessed by
153 monitoring COD.⁸ Cyclic voltammetry technique was employed to observe redox variations
154 in bio-electrochemical behaviour of the biocatalyst under three different experimental setups
155 using potentiostat-galvanostat system. A potential ramp of +0.5 to –0.5 V was applied at a
156 scan rate of 30mV/s to record the voltammograms. All the electrochemical assays viz.,
157 derivative cyclic Voltammogram (DCV), Tafel plots, slopes (β_a and β_c) and polarization
158 resistance (R_p) were deduced from the Voltammetric studies.¹⁶ All the analyses were
159 performed in triplicates and the mean values were plotted in the graphs.

160

161

162

163

164 3. Results and Discussions

165 3.1 Colour Removal

166 Initially, all the three bioreactors (BET, AnT and control) were optimized with DSW at an
167 organic loading rate (OLR) of 1.36 kg COD/m³-day (without dye) for 10 cycles (HRT, 48 h)
168 to facilitate the biomass growth. After stabilization with respect to substrate removal, the
169 bioreactors were subsequently fed with SDW (azo dye load, 50 mg /l) and operated
170 continuously for 15 cycles. Azo dye removal efficiency was evaluated for all the three
171 reactors, wherein BET documented decolourization of 52% followed by AnT (32%) and
172 control (3%) during initial period of operation (3rd cycle) (Fig.1). With increase in number of
173 cycles, the decolourization efficiency was observed to increase gradually (BET and AnT) and
174 maximum performance was observed at 15th cycle of operation which is attributed to the
175 acclimatization of biocatalyst. BET documented higher colour removal efficiency (70 %)
176 accounting to a dye removal of 35 mg dye/l, which is relatively higher than the AnT (42%; 21
177 mg dye/l removal) and control (2.44%; 1.22 mg dye/l removal) operations.

178

179

Fig. 1

180 3.1.1 UV-Vis Spectral Scan

181 Decolourization pattern of azo dye was observed under static condition with multi-scan
182 spectrum analysis (200-800 nm) using UV-visible spectroscopy at regular time intervals for
183 all the three reactors (Fig. 2a). Two peaks were observed in UV region near the spectral
184 ranges of 500 to 700 nm and 320 to 360 nm. The intense peak at 618 nm corresponding to
185 chromophore (-N=N-) and peak at 340 nm is associated with the presence of oxidized
186 aromatics such as phenolic and naphthoquinone compounds.^{14,15} The peaks at 340 nm
187 increased with operation time indicating the accumulation of amines under reductive
188 microenvironment which was observed to be similar in all the three reactors. Among three
189 reactors, UV-Vis spectrum of BET reactor at various time intervals clearly portrayed the
190 decrement in peak height at 618 nm depicting the degradation of dye into corresponding
191 intermediates.⁴ Less absorbance was observed at 48 h, illustrating the reduction of
192 chromophores by the electrons liberated in the reactor. The self-induced bio-potential
193 developed in BET system was able to cleave the azo dye compounds towards enhanced dye
194 degradation. Subsequently, AnT also showed decrement in the peak height indicating
195 effective reductive behaviour in anaerobic conditions, which might have resulted due to the

196 increase in the amount of aromatic amines.⁷ The shift in wave length in the UV-scan indicates
197 the biochemical interface of dye which is consistent with azo bond cleavage and
198 transformational changes to the aromatic structure. In control operation, the decrement in
199 peak height was not observed indicating that the chromophores were not cleaved due to the
200 absence of biocatalyst. In BET operation, the peaks corresponding to 6h and 12h at 340nm
201 increased with time depicting the accumulation of aromatic amines and decreased at 24h to
202 48h depicting the degradation of aromatic amines to lower molecular weight aliphatic
203 hydrocarbons. BET can be considered more favourable than AnT for the treatment of azo
204 based wastewater due to the development of high density electroactive species on the anode
205 with faster electron transfer rate which might be used for the electrochemical substitution and
206 electrolytic dissociation of complex compounds.

207 The disparity in treatment efficiency is attributed to the capability of biocatalyst to undergo
208 metabolic shift with regard to the experimental conditions. The presence of electrode
209 assembly as well influenced the performance in BET compared to the AnT system. In the
210 control operation, removal efficiency was almost negligible and the dye concentration
211 remained almost similar until the end of operation. In AnT system, azo dye is degraded by
212 bacteria through reductive enzymatic cleavage of azo bond which acts as an electron acceptor
213 under anaerobic condition.⁷ However, in BET system, the presence of solid electron acceptor
214 influenced the effective degradation of the complex dye molecules faster than the
215 conventional anaerobic treatment process due to the enrichment of electrochemically active
216 bacteria (EAB).

217

218 Fig. 2a

219 3.2 Substrate Degradation

220 Initially, the bioreactors were fed with DSW (without dye) at an OLR of 1.36 kg COD/m³-
221 day and operated for 6 cycles with a HRT of 48 h. Subsequently, the reactor was fed with
222 synthetic azo dye bearing wastewater (50 mg dye/l) and operated for 15 cycles. Higher
223 substrate degradation was observed in BET (85%; SDR: 1.15 kg COD/m³-day) followed by
224 AnT (75%; 0.78 kg COD/m³- day) and Control (2.9%; 0.04 kg COD/m³- day) without dye
225 addition, which indicates the rapid metabolic capabilities of bacteria in utilizing glucose as
226 co-substrate and abiotic-control resulted in negligible performance (Fig. 2b). After
227 subsequent dye addition, lower substrate degradation was observed in both BET (3rd cycle:
228 55%) and AnT reactors (3rd cycle: 35%) and observed to increase with increase in cycle

229 operation which is attributed to the non adaptability of bacteria to dye environment.
230 However, increased COD removal efficiency with additional cycles is due to the adaptable
231 nature of biocatalyst in utilizing dye molecule rapidly. Maximum substrate removal was
232 observed at 15th cycle in BET (79.5%) followed by AnT (48%) and Control (2.33%). Carbon
233 sources have an important influence on dye degradation because azo dyes are deficient in
234 carbon and require co-substrate for the breakage of the azo bond, energy for the growth,
235 survival of the microorganisms and as electron donors.¹⁷

236 The requirement of simple carbon source is inevitable for dye degradation.¹⁰ Apart from the
237 sole substrates of recalcitrant dyes in anode chamber, co-metabolism using simple substrate
238 (glucose) provides a good candidate for bioremediation of these recalcitrant azo
239 compounds.¹⁸⁻²⁰ The mechanism of co-metabolism involves the liberation of reducing powers
240 which can be utilized for the degradation of dye molecules as terminal electron acceptors
241 with the help of *in situ* mediators produced during the process. The dye molecules and its
242 reduced intermediates also act as mediators during the operation and enhance the electricity
243 generation and substrate removal in BET system. The substrate removal is expressed in terms
244 of SDR and the removal efficiency varies with respect to reactor operation in the experiment.
245 The substrate degradation rate (SDR) was observed to be higher in BET (1.0789 kg COD/m³-
246 day) followed by AnT (0.653 kg COD/m³-day) and Control (0.032 kg COD/m³-day). It is
247 clear evidence that BET operation depicted 1.7 folds higher substrate degradation efficiency
248 than AnT due to the advantage of self-induced bio-electro catalytic microenvironment and
249 enabled electron acceptor dependent respiration. The anodic electron flux reactions might
250 have also played a role in enhancing the substrate degradation in BET operation.²¹ The use of
251 biocatalyst, presence of *in situ* mediators and the type of metabolism (co-metabolism) may
252 potentially affect the degradation pathways of azo dye substances.^{18,22}

253 **Fig. 2b**

254 **3.3 Enzymes Activity**

255 **3.3.1 Azo reductase Activity**

256 The cleavage of azo bonds catalyzed by azo reductase enzyme with the aid of an electron
257 donor (NADH and/or NADPH) was monitored with respect to time (BET, AnT and control
258 reactors) (Fig.3a). At initial cycles of operation, lower azo reductase activity was observed
259 for all the three reactors and gradual improvement in the enzyme activity was observed
260 during the due course of operation. Maximum enzyme activity was observed at 15th cycle of

261 operation in BET (26.2 ± 1.2 U) followed by AnT (18.9 ± 0.9 U) and abiotic control ($0.15 \pm$
262 0.05 U). Azo reductase enzyme plays a major role to cleave -N=N- bond of azo dyes into
263 colorless metabolites analogous to the aromatic amines. The azo reductase enzyme consumes
264 NADH and/or NADPH as an electron donor and dye as an artificial electron acceptor to
265 cleave the bond. The conversion of NADH to NAD liberates the reducing powers that are
266 used for the reduction of azo dyes to aromatic amines via hydrazines formation.²³ The dye
267 degradation evidenced in this study is attributed through two main routes viz., symmetrical
268 and asymmetrical cleavage of azo bond, where the typical microbial metabolism with respect
269 to the available carbon source (glucose and dye) might have contributed for the generation of
270 reducing powers.^{24,25} In AnT system, presence of redox mediators such as NAD/NADH
271 accelerate the decolorization rate of azo dyes by shuttling electrons between biological
272 oxidation of primary electron donor to electron acceptor such as azo dye.²⁶ Besides,
273 NAD/NADH in BET system, the presence of electrode assembly develops the self driven
274 redox mediators to enhance the dye degradation. The dye removal pattern correlates well with
275 the azo reductase enzyme indicating a major role of enzyme playing in the cleavage of azo
276 compounds. Stable enzyme activity with each feed event in both the bioreactors supports the
277 robustness of systems in dye reduction.^{4, 10}

278

279

Fig. 3a

280 3.3.2 Dehydrogenase Activity

281 Dehydrogenase (DH) belongs to oxido-reductase group of enzymes catalyzing the redox
282 reactions for the inter-conversion of metabolites and also helps in shuttling the protons (H^+)
283 between metabolites with the help of electron carriers (NAD^+ , FAD^+ , etc).²⁷ They play a
284 crucial role in dye degradation to its intermediates by catalyzing the proton transfer from the
285 substrate or intermediates to the dye molecules. Higher DH activity was observed with BET
286 operation ($2.6 \mu\text{g/ml}$), followed by AnT ($1.4 \mu\text{g/ml}$) and control ($0.07 \mu\text{g/ml}$) (Fig.3b). DH
287 enzyme activity represents metabolic activities of the microorganism and can be considered
288 as a good measure of microbial oxidative activities.²⁸ BET showed relatively higher enzyme
289 activity when compared to other operations because the electroactive consortia developed in
290 BET is robust to oxidize complex substrates indicating higher metabolic activity of self-
291 immobilized bacteria on the working electrode. It can also be hypothesized that high DH
292 activity in the BET reactor was due to close proximity of electron donors and acceptors thus
293 facilitating rapid electron transfer compared to AnT operation. Proton shuttling between the

294 intermediates during metabolic activity might also be involved in the dye reduction. It is clear
295 that the increased enzyme activities are proportional to dye degradation and electrogenic
296 activity which might have stimulated the metabolic and enzyme activities of the biocatalyst
297 robust to the subjected microenvironment.

298 **Fig. 3b**

299 **3.4 Self Induced Electrogenesis**

300 BET depicted biogenic electricity production along with concomitant azo dye removal.
301 Initially the reactors were fed with DSW (with no dye addition) at an OLR of 1.36 kg
302 COD/m³-day and operated for 10 cycles with a HRT of 48 h. Maximum OCV of 365 mV and
303 PD of 100 mW/m² were observed at 10th cycle in BET system, while the control reactor
304 documented OCV of 58 mV (abiotic) (Fig.4a). The results clearly indicate the influence of
305 biocatalyst in BET system, which facilitated higher biomass growth, documenting higher
306 bioelectrogenic performance than control. The reactors were further fed with synthetic azo
307 dye bearing wastewater (SDW-50 mg/l) and operated continuously accounting for total time
308 of 720 h with an OLR of 1.36 kg COD/m³-day. Both the systems showed a drop in
309 performance during initial cycles (Cycle 1-BET-OCV: 130 mV and PD: 12 mW/m²; Control:
310 OCV:20 mV and PD: 0.12 mW/m²) which might be due to the inhibitory effect of toxic dye.
311 With increase in cycles, a gradual increment in performance was observed in BET system.
312 During 8th cycle, BET documented OCV of 200 mV and PD of 40 mW/m² and control reactor
313 documented OCV of 48 mV (0.41 mW/m²). The performance of control reactor was almost
314 similar to that of without dye operation, since reducing equivalents that degrade dye
315 molecules are not liberated due to the absence of biocatalyst. However, the electrogenesis
316 observed in the control operation might be because of the potential produced by electrode
317 assembly. The reactors were operated continuously for 15 cycles and a stabilized
318 performance was observed from 12th cycle and depicted maximum electrogenesis. In BET
319 system, a stable voltage of 350 mV and PD of 85 mW/m² was observed at 15 cycle of
320 operation indicating the acclimatization of the biocatalyst. The organic and inorganic
321 substrates present in the azo dye based wastewaters were oxidized by the bacteria producing
322 excess of electrons (e⁻) and protons (H⁺) in the anode chamber. The reducing equivalents
323 generated in the system were partially used to harness electricity and partially used to cleave
324 the azo bonds of the dye that acts as alternate electron acceptor (dye molecules) present in
325 wastewater which favoured the breakage of chromophores in the anode chamber. Besides the

326 benefits of power generation, the reduction of azo dyes is accomplished through
327 bioelectrochemical reduction without the application of external power source.^{16, 29} On the
328 contrary, abiotic-control depicted no increase in power generation due to the absence of
329 biocatalyst (OCV- 50 mV; PD - 0.5 mW/m²).

330

Fig. 4a

331 3.4.1 Anode potential

332 Variations in anode potential against external resistance (30k Ω to 50 Ω) were recorded against
333 saturated Ag/AgCl (S) electrode during both BET and control operations (Fig.4b). Maximum
334 open circuit anodic potential was -350 mV for BET system and -50 mV for control system
335 with the absence of resistor. Higher anode potential indicates transfer of more energy for
336 microbial growth and cell maintenance due to the availability of substrate in BET system.³⁰
337 Although substrate availability was same in the control system the degradation of substrate
338 was not observed due to the absence of biocatalyst. Operation for longer period (15 cycles) in
339 BET system favours effective growth of electrochemically active bacteria on the anodic
340 electrode. The formation of biofilm on the electrode and the absence of membrane reduce
341 internal losses documenting higher anode potential in BET system. In BET system, anode
342 potential varied between -312 to -175 mV with varying resistor of 30 and 0.05 k Ω . The
343 potential was observed to drop from 5 k Ω in BET reactor and 0.5 k Ω in control reactor,
344 suggesting the possibility of effective electron discharge at the respective resistors. The
345 electrochemically active consortia will have higher membrane potential, which helps in
346 delivering electrons against the anode potential. The induced electrochemical oxidation
347 during electrogenesis as well as the simultaneous bio-electrochemical reactions might have
348 helped in transferring the electrons to dye molecules, resulting in the decolorization of
349 wastewater.

350 3.4.2 Cell electromotive force

351 Polarization behaviour of the electrodes was observed by varying the resistances (30 to 0.05
352 k Ω) at 15th cycle of operation for BET and control reactors (Fig.4b). In BET operation, the
353 potential at 30 k Ω was 380 mV and observed to decrease with decrease in resistance (0.05 k Ω
354 - 192 mV). The voltage profile indicates that, until 5 k Ω the flow in potential was restricted
355 and observed to drop gradually until 1 k Ω and dropped drastically from 0.5 k Ω .
356 Correspondingly, current density (450 mW/m²) increased with decrease in resistors indicating

357 the flow of electrons. The self-immobilized biofilm developed on the anode surface of the
358 BET system showed marked influence on both bioelectricity production and substrate
359 degradation efficiency. In the case of abiotic control operation, the performance was very low
360 due to the absence of biocatalyst. Generally, the microbes that acts as the biocatalyst have
361 high electron discharge capability and are considered to be electrochemically active and are
362 crucial in the BET operation. Maximum power density of 80 mW/m^2 was observed at cell
363 design point (CDP) of 100Ω with corresponding current density of 381 mA/m^2 in BET
364 performance.

365 **Fig. 4b**

366 **3.5 Bioelectrochemical Behaviour**

367 **3.5.1 Cyclic Voltammetry**

368 The bioelectrochemical redox transition coupled to catalytic oxidation and reduction
369 behaviour was analyzed for all the three reactors for every 6 hr interval (Fig. 5a). Maximum
370 redox catalytic currents were observed in BET system (oxidative current, OC: 39.6 mA and
371 reductive current, RC: -19.5 mA) followed by AnT (OC: $6.2 \pm 0.2 \text{ mA}$; RC: $-7.1 \pm 0.15 \text{ mA}$)
372 and control (OC: $0.326 \pm 0.1 \text{ mA}$; RC: $-0.586 \pm 0.2 \text{ mA}$). OC was higher than RC in BET
373 system indicating that the redox behaviour is more favourable towards oxidation due to the
374 development of electrogenic microenvironment that develops a continuous stress on the
375 selectively enriched electrochemically active consortia facilitating on the anode surface by
376 mediating higher electron transfer rate.²⁹ However, BET operation resulted higher redox
377 currents than AnT and control operation due to the effective contact of biofilm for efficient
378 electron transfer, minimization of mass transfer losses as well as for the involvement of dye
379 molecule itself as a mediator. In AnT system, the increment in reduction current is ascribed to
380 the increased reduction reactions towards the breakdown of dye into reduced intermediates
381 and its persistent accumulation.⁷ Control operation showed a very less catalytic current due to
382 the absence of biocatalyst. The redox catalytic currents observed in BET system was well
383 correlated with the higher COD and dye removal, enzyme activities during the reactor
384 operation.

385 Voltammogram also depicts the redox mediators involved to alleviate the shuttling reactions
386 between the electron donor and acceptor. When the redox potential of a mediator equals the
387 applied potential, the peaks were deducted indicating the presence of mediators for electron

388 transfer.^{31, 32} Distinct peaks were observed in BET operation, with respect to time different
389 interval. The peak potentials detected are -0.164 V (6 h), 0.32 V and 0.258 V (12 h), 0.27 V
390 (24 h), -0.235 V (36 h) and 0.431 V (48 h) which might correspond to the bacterial membrane
391 bound proteins viz., Fe-S proteins, NAD/NADH, Cytochrome-bc1, Cytochrome-C,
392 Flavoproteins and NO₃/NO₂ respectively.³¹ The presence of electrode assembly in BET
393 system enables the enrichment of ARB on electrode surface that transfer electrons via the
394 observed membrane bound proteins. The cytochrome-C complex present in almost all the
395 bacterial species acts as an electron carrier which helps in the efficient direct electron transfer
396 and the NO₃/NO₂ detected is the dye intermediate formed at the end of cycle operation
397 depicting the breakdown of dyes into simple non toxic compounds. The electrode assembly is
398 the integral part of the BET system that acts as a solid electron acceptor. The involvement of
399 these mediators and membrane bound proteins is in correlation to the higher redox currents
400 attributing its role in dynamic electron flux in BET operation.

401 **3.5.2 Derivative Cyclic Voltammetry (DCV)**

402 The derivative Voltammogram represents the rate of change of voltammetric current with
403 respect to time and electrode potential E (di/dt). The numbers of peaks were comparatively
404 higher in DCV than the corresponding CV analysis. The derivative of CV helps to find the
405 EET site of the redox mediator involved in the process in the form of a peak in both BET and
406 AnT operations (Fig.5b). However, numbers of peaks were comparatively higher in BET
407 system than the corresponding AnT operation. In BET system, two reversible peaks were
408 detected at -0.165 V and 0.188 V corresponding to the involvement of Cytochrome-bC1 and
409 Fe-S proteins respectively. In addition, five quasi reversible peaks were detected at -0.188 V,
410 0.035 V, -0.141 V, 0.023 V and -0.094 V which correspond to the involvement of Fe-S
411 proteins, Quinones and Cytochrome bC1 respectively. In the case of AnT operation, six quasi
412 reversible peaks were detected, each with a potential of 0.141 V, 0.094 V, -0.129 V, 0.177 V,
413 0.011 V and -0.117 V corresponding to the involvement of Cytochrome-bC1 and Fe-S
414 proteins respectively. All the redox mediators detected during DCV analysis are the
415 membrane bound proteins of bacteria that act as electron carriers during the process.
416 However, detection of quinones as redox shuttlers in BET system implies the direct evidence
417 of dye degradation mechanism which forms the aromatic derivatives. Quinones are the
418 secondary intermediates formed during the degradation of aromatic compounds such as dye
419 molecules which serves as electron carriers/ acceptors during the process. This additional
420 advantage of quinone as redox mediator in BET system proves the effective dye degradation

421 compared to other two reactors. On the contrary, control operation did not show any peaks
422 which might be attributed to the absence of biocatalyst activity.

423

Fig. 5

424 3.5.3 Charge

425 Charge distribution was observed to vary during the anodic oxidation and cathodic reduction
426 with the function of biocatalyst and electrode assembly. Charge distribution obtained from
427 the voltammetric profiles was observed to be higher for BET than AnT and control operations
428 (Sfig1). At initial period of operation (0 h) the charge was observed to be 0.64 C which
429 increased with time (6 h; 0.89 C) and gradually decreased to 0.804 C until 36th h and random
430 drop was observed at 48th h (0.671C). This depicts the rapid oxidation of substrate and co-
431 substrate at the initial hours of cycle operation and hence the electron availability on the
432 working electrode is higher which yields the elevated power in BET operation. In case of
433 AnT operation, initial operation (0 h) documented 0.167 C which changed marginally with
434 respect to cycle operation (6 h, 0.173 C; 12 h, 0.187 C; 24 h, 0.176 C) with a relative rapid
435 drop at 36 h (0.158 C). The absence of electrode assembly in AnT system indicates the non-
436 adaptation of electrochemically active biomass in the reactor resulting in low performance
437 than BET system. In the control operation, negligible charge of ≈ 0.003 C was observed due
438 to the absence of biocatalyst as well as electrode assembly. Almost eight fold higher charge
439 distribution was observed with BET when compared to AnT which might be attributed to the
440 variation in the relevant energy levels of the biocatalyst, participation of the soluble redox
441 species and electron transfer efficiencies. Charge separation can also be expressed in terms of
442 capacitance with respect to the voltage applied. Higher capacitance was observed with BET
443 (1.76 F; 6 h) followed by AnT (0.37 F; 12 h) and Control operation (0.03 F; 48 h) which
444 correlates with the distribution of charge, indicating that the electron holding capability of
445 biocatalyst was higher with the conjunction of biocatalyst and electrode assembly in BET.
446 As charge is directly proportional to capacitance, increase in charge also concurrently
447 increases the capacitance that indicates higher availability of electrons due to the inter-
448 conversion of metabolites at higher substrate load. The energy (J) generated and number of
449 electrons (n) during potential sweep also followed a similar pattern as charge and capacitance
450 with respect to time intervals. The energy stored and number of electrons is higher with BET
451 operation at 6 h (0.45 J; 5.6×10^{18}) compared to AnT (12 h, 0.094 J; $1.179.18 \times 10^{18}$). This
452 higher energy stored and number of electrons generated depicts the optimization of
453 bioelectrogenic biomass for the higher electrogenic activity and dye removal in BET than

454 AnT depicting the robustness of bioelectrogenic bacteria in dye removal and electricity
455 generation in BET system.

456

SFig. 1

457 3.5.4 Tafel Slopes

458 Tafel plots provide a visual understanding of the electron losses present in the system and
459 help to interpret the biocatalytic activity based on the derived kinetic parameters viz.,
460 oxidative Tafel slope (β_a), reductive Tafel slope (β_c) and polarization resistance (R_p) (Fig.6).
461 Tafel analysis depicted a marked variation in all the three systems viz., BET, AnT and abiotic
462 control operations during oxidation and reduction reactions.

463 Reduction slopes (β_c) were comparatively lower than the oxidation slopes (β_a) in all the three
464 systems which indicate the feasibility of effective neutralization/reduction of dye molecules
465 in the system. In BET operation, the reductive slope of 0.165 V/dec (0 h) decreased to 0.1
466 V/dec till 24 h and slightly increased to 0.12 V/dec and 0.14 V/dec at 36 and 48 h
467 respectively. The decrement in reduction slope till 24 h depicts the scope of reduction
468 reactions in the bioreactor and further enhances the breakage of chromophore groups,
469 whereas the oxidative slope of 0.53 V/dec (0 h) decreased slightly to 0.5 V/dec (12 h) and
470 again showed slight increment till the end of cycle operation and visualized 0.62 V/dec (48
471 h). This is attributed to the influence of electrode assembly coupled with biocatalyst activity
472 that induces the bioelectrogenic micro environment in the system to carry out the oxidation
473 reactions at a higher rate. Degradation of dye molecule was found to be higher in BET system
474 which is in accordance with the observed low oxidation slope and COD removal. Higher
475 oxidation indicates the liberation of more number of redox equivalents to perform effective
476 dye degradation process. Degradation of dye molecule leads to the liberation of aromatic
477 amines (intermediates) which further acts as redox shuttles in the electron transfer. But in the
478 case of AnT operation, the reduction slopes were little lower when compared to BET
479 operation depicting the higher reduction activity of dye molecules. The reduction slopes
480 which were little lower till 6 h (0.6 V/dec) showed nominal increment till 36 h (0.1 V/dec)
481 and visible shift was observed at 48 h (0.18 V/dec) depicting the dye reduction was higher
482 during the initial hours of cycle operation in AnT, whereas the oxidative slopes showed
483 nominal decrement from 1.12 V/dec (0 h) to 0.7 V/dec (48 h) till the end of cycle operation
484 with respect to the time intervals illustrating the utilization of carbon and dye as electron
485 donors until the end of cycle operation. Abiotic-control illustrated higher redox slopes as
486 there is no biocatalyst to perform redox reactions.

487 Polarization resistance (R_p), derived from Tafel analysis, refers to the resistance offered
488 towards electron transfer from the biocatalyst to the electrode. R_p was found to be lesser in
489 BET operation when compared to AnT and abiotic-control. Highest resistance was offered by
490 control operation (7000 Ω ; 0 h) followed by AnT (97 Ω ; 48 h) and BET (30 Ω ; 0 h). This
491 lower resistance in BET could be the probable reason for higher dye degradation and more
492 enzymatic activity. Low resistance present in the BET and AnT systems minimizes losses and
493 provides effective electron transfer between substrate and the dye molecule and thus
494 enhances the dye removal.

495 **Fig. 6**

496 **3.6 Electron Acceptor-Dependent Respiration**

497 In BET, electron acceptors are of crucial importance as the terminal reduction reactions are
498 dependent upon the availability of terminal electron acceptors for the degradation of
499 wastewater/pollutants. The electron acceptors respired by bacteria often have solid and
500 soluble forms that typically coexist in the bioreactor environment.³³ In the present study, BET
501 system functioned with coupled action of electrode assembly as solid electron acceptor as
502 well as bacteria as biocatalyst documented significant dye remediation with simultaneous
503 power generation in comparison to the corresponding AnT and abiotic-control operations
504 (Table 1). ARB present in BET system would respire on the electrode surface by utilizing the
505 solid electrode as electron acceptor, thereby enhancing the dye degradation and power
506 generation efficiency of the system. The present study elucidates the significant role of solid
507 electron acceptor in conjunction with biocatalyst for dual benefits of power generation with
508 simultaneous dye reduction. Direct electron flux between a microbe and a solid phase is a
509 widespread and environmentally significant process.^{33,34} Using solid electrodes as electron
510 acceptors enables efficient electron transfer between biocatalyst and anode during dye
511 degradation process in BET. During BET operation, two overlapping mechanisms might
512 occur for coordinating extracellular electron transfer to solid phase electron acceptors viz.,
513 direct cell-electrode contact with bacterial outer membrane bound cytochromes serving as
514 reductases as well as dye molecules functioning as electron shuttles. BET system visualized
515 dual electron transfer mechanisms viz., direct and mediated. Voltammetric analysis depicted
516 the involvement of outer membrane bound cytochromes, flavoproteins, Fe-S proteins and
517 quinones that are responsible for DET to the solid electron acceptor (electrode) in BET
518 system. DET mechanism is possibly done by the ARB present on the electrode surface. The
519 organic fraction of wastewater will be utilized by the bacteria present in suspension as well as

520 in biofilm and will liberate the reducing equivalents towards the electrode. During the BET
521 operation, electrode assembly induces the development of potential difference by the
522 biocatalytic action of electrochemically active bacteria enriched around the electrodes in
523 carrying out the simultaneous redox reactions towards the breakdown of dye molecules.
524 Besides, the breakdown of complex dye molecule results in the generation of reduced dye
525 intermediates that in turn acts as redox mediators/electron shuttles during the transfer of
526 electrons to the solid electron acceptor/ for the other dye molecule reduction enabling the
527 mediated electron acceptor.^{4,34,35} Bio-electrogenic activity enhanced when bacterial
528 respiration was coupled with the electrode assembly in treating/utilizing the azo dye based
529 wastewater which can be attributed to the electron acceptor-dependent respiration.³⁶
530 Comparative analysis between three reactors during the study depicts the significant
531 influence of biocatalyst and electrode assembly in BET system towards higher color removal
532 (79.5 %), power generation (85 mW/m²), electron transfer mechanism, redox catalytic
533 currents (39.6 mV), azo reductase (26.2 U) and DH activity (2.6 µg/ml of Toluene) in
534 comparison to AnT and abiotic control systems. On the contrary, abiotic control system
535 lacking biocatalyst resulted in poor/no dye degradation in comparison to respective systems
536 operated. AnT operation (with biocatalyst and without electrode assembly) resulted in poor
537 azo dye degradation, enzymatic activities as well as redox catalytic currents. In general, the
538 terminal reduction reactions are dependent upon the hierarchy of the most electronegative
539 species/solid electron acceptor existing in the surrounding microenvironment. Absence of an
540 electron acceptor results in inter species electron transfer, where the electrons liberated by
541 one microbe will get utilized by another bacteria towards its growth and metabolic
542 activities.³⁷ However, voltammetric analysis during AnT operation documented the
543 involvement of membrane bound cytochromes and flavo proteins during the electron transfer,
544 where the mixed bacterial population would have utilized these in transferring the electrons
545 among the inter species. The results obtained during the study provide new insights into the
546 bacterial respiration during BET operation utilizing various electron acceptors viz., electrodes
547 as well as dye intermediates that enhanced the dye degradation efficiency with simultaneous
548 power generation.

549

Table 1

550

551

552 4. Conclusion

- 553 • The effect of electrode as solid electron acceptor and bacteria as biocatalyst
554 documented significant and specific process efficiency towards dye degradation with
555 simultaneous power generation in BET system compared to the corresponding AnT
556 and abiotic-control systems.
- 557 • The self induced bio-potential developed in BET system as a result of electrode
558 assembly stimulated enrichment of electrochemically active bacteria that discharge
559 higher number of reducing equivalents towards dye degradation and power
560 generation.
- 561 • Two overlapping mechanisms for electron transfer were observed during BET
562 operation, where ARB contributed for DET via cytochromes, flavo proteins towards
563 the electrode (anode) and the reduced dye intermediates functioned as electron
564 shuttle/mediator for other dye molecule reduction/electrode surface.
- 565 • Absence of electrode assembly in AnT and bacteria in abiotic-control system
566 respectively, resulted in poor system performance in terms of azo dye degradation,
567 azo reductase activity, colour removal, DH activity as well as redox catalytic currents
568 depicting the lack of concurrence between the biocatalyst and solid electron acceptor
569 in both AnT and abiotic-control systems.
- 570 • The study clearly documented that the presence of electrode assembly and the
571 anaerobic consortia as biocatalyst in a system procures the advantage of electron
572 acceptor dependent respiration offering dual benefits of dye degradation and power
573 generation.

574 Acknowledgments

575 The authors wish to thank the Director, CSIR-IICT for support and encouragement in
576 carrying out the research. The authors would like to acknowledge DBT for providing
577 National Bioscience Award research grant, SETCA, (CSC-0113) and New INDIGO project
578 (DST/IMRCO/New INDIGO/Bio-e-MAT/ 2014/(G/ii)). CNR, JAM and GV duly
579 acknowledge CSIR for providing the research fellowship.

580

581

582

583 **References**

- 584 1. P. Nigam, I.M. Banat, D. Singh and R. Merchant, *Process Biochem.*, 1996, 435-442.
- 585 2. Z. Aksu, *Process Biochem.*, 2005, 40, 997-1026.
- 586 3. A.N Kumar, C.N Reddy, S.V Mohan, *Bioresour Technol*, 2015, 56-64.
- 587 4. C. Nagendranatha Reddy, A. Naresh Kumar, J. Annie Modestra, and S. Venkata
588 Mohan, *Bioresour. Technol.*, 2014, 165, 241-249.
- 589 5. S.Venkata Mohan, N.C.Rao, P.N.Sarma. *Ecological Engineering*, 31, 242-250.
- 590 6. N.C.Rao, S.Venkata Mohan, P.Muralikrishna, P.N.Sarma. *J. Hazard.Mat.* 124, 59-67
- 591 7. S. Sreelatha, C. Nagendranatha Reddy, G. Velvizhi, and S. Venkata Mohan, *Bioresour*
592 *Technol*, 2015, 188, 1-2.
- 593 8. APHA, 1998. Standard methods for the examination of water and wastewater, 20th ed.
594 American Public Health Association/American water works. Association/Water
595 environment federation, Washington DC, USA.
- 596 9. S. Venkata Mohan, G. Velvizhi, K. Vamshi Krishna and M. Lenin Babu, *Bioresour*
597 *Technol*, 2014a, 165, 355-36.
- 598 10. S. Venkata Mohan, P. Suresh Babu and S. Srikanth, *Sep. Purf. Technol*, 2013a, 118,
599 196-208.
- 600 11. Y. D. Kumar, J. Srinivas, G.Velvizhi, A.N. Kumar, Y.V. Swamy, S. Venkata Mohan,
601 *Bioresour Technol*, 2015, 188, 33-42.
- 602 12. K. Rabaey, G. Lissens and W. Verstraete, 2005a; 375-396.
- 603 13. D. R. Lovley, *.Nat Rev Microbiol*, 2006a, 4, 497-8.
- 604 14. A. Naresh Kumar, C. Nagendranatha Reddy, R. Hari Prasad and S. Venkata Mohan,
605 *Water Res*, 2014, 60, 182-196.
- 606 15. S. Venkata Mohan, C. Nagendranatha Reddy, A. Naresh Kumar, and J. Annie
607 Modestra, *Bioresour. Technol*, 2013b, 147, 424-433.
- 608 16. G. Velvizhi and S. Venkata Mohan, *Water Res*, 2015, 70, 52-63.

- 609 17. H. Yemendzhiev, Z. Alexieva and A. Krastanov, *Biotechnol Biotec*, 2009, 23, 1337-9.
- 610 18. L. Huang, S. Cheng and G. Chen, *J Chem Technol Biotechnol*, 2011, 86, 481-491.
- 611 19. C. Zhang, G. Liu, R. Zhang and H. Luo, *J Environ Sci Health*, 2010, Part A. 45, 250-
612 256.
- 613 20. Y. Cao, Y. Hu, J. Sun and B. Hou, *Bioelectrochemistry*, 2010, 79, 71-76.
- 614 21. G. Mohanakrishna, S. Venkata Mohan and P.N. Sarma, *J. of Hazardous Materials*,
615 2010, 177 (1), 487-494.
- 616 22. F. Aulenta, A. Canosa, M. Majone, S. Panero, P. Reale and S. Rossetti, *Environ Sci*
617 *Technol*, 2008, 42, 6185-6190.
- 618 23. A. Pandey, P. Singh and L. Iyengar, *Int. Biodeterior. Biodegrad*, 2007, 59, 73-84.
- 619 24. S. Moosvi, X. Kher and D. Madamwar, *Dyes Pigm*, 2007, 74, 723–729.
- 620 25. C.I. Pearce, J.R. Lloyd and J.T. Guthrie, *Dyes Pigm*, 2003, 58, 179-196.
- 621 26. J. Kunal, S. Varun, C. Digantkumar and D. Madamwar, *J. of Haz. Mat*, 2012, 378-386.
- 622 27. S. Sun, G. Zhiguo, R. Yang, Z. Sheng and P. Cao, *Afr. J. Biotechnol*, 2012, 11, 7055-
623 7062.
- 624 28. T. Griebe, G. Schaule and S. Wuertz, *J. Ind. Microbiol. Biotechnol*, 1997, 19, 118-122.
- 625 29. G. Velvizhi and S. Venkata Mohan, *Bioresour. Technol*, 2011, 102, 10784-10793.
- 626 30. S. Srikanth, S. Venkata Mohan and P. N. Sarma, *Bioresource Technology*, 2010, 101,
627 5337-5344.
- 628 31. M. T. Madigan and J. M. Martinko, *Brock Biology of Microorganisms*, 11th ed.;
629 Pearson Prentice Hall: Upper Saddle River, NJ, 2006.
- 630 32. J. Annie Modestra and S. Venkata Mohan, *RSC Adv*, 2014, 64, 34045–34055.
- 631 33. Y. Yang, Y. Xiang, G. Sun, W. Wu and M. Xu, *Environ. Sci. Technol*, 2015, 49,
632 196–202.
- 633 34. J. S. Deutzmann, M. Sahin and A. M. Spormann, *mBio*, 2015, 6, 496-15.

- 634 35. S. T. Lohner, J. S. Deutzmann, B. E. Logan, L. Leigh and A. M. Spormann, ISME J
635 2014, 8, 1673–1681
- 636 36. E. A. Rotaru, M. S. Pravin, F. Liu, L. Anghua, B. M. Markovaite, S. Chen, K. Nevin
637 and D. Lovely, Appl. Environ. Microbiol, 2014, doi:10.1128/AEM.00895-14.
- 638 37. V. B. OLiveria, M. Simoes, L. F. Melo and A. M. F. R. Printo, Biochem Eng J, 2013,
639 73,53-64.

640 **Table. 1 Comparative performance of BET, AnT and Abiotic Control reactors**

S. No	BET	AnT	Abiotic
Color (%)	70	42	2.4
COD (%)	79.5	48	2.33
OCV (mV)	350	-	50
PD (mW/m ²)	85	-	0.5
Azoreductase Activity (U)	26	18.9	0.15
DH (µg/ml of Toluene)	2.6	1.4	0.07
Oxidation Currents mV	39.6	6.2	0.326
Reduction Currents - mV	-19.5	-7.1	-0.586
β _a (V/dec)	0.599 (36 h)	1.097 (0 h)	0.841 (24 h)
β _c (V/dec)	0.164 (0 h)	0.171 (48 h)	0.197 (0 h)
R _p (Ω)	31 (0 h)	112 (48 h)	7373 (0 h)
CV mediators	Fe-S proteins, NAD/NADH, Cyt bc1, Cyt C, Flavoproteins and NO ₃ /NO ₂	Cyt C and Flavoproteins	-
DCV Mediators	Fe-S proteins, Quinones and Cyt bc1	Cyt-bC1 and Fe-S proteins	-
Charge (C)	0.89 (6 h)	0.19 (12 h)	0.0147 (48 h)
Capacitance (F)	1.76 (6 h)	0.37 (12 h)	2.91E-02 (48 h)
Energy Stored (J)	0.45 (6 h)	0.094 (12 h)	7.42E-03 (48 h)
No. of electrons (n)	5.5638E+18 (6 h)	1.1684E+18 (12 h)	9.18E+16 (48 h)
Reference	Present Study	Sreelatha et al., 2015	Present Study

641

Captions for Figures

Fig 1: (a) Variation in enhancement of overall color removal efficiency in BET, AnT and abiotic-control bioreactors with 15 cycles operations (b) Relative variation of color removal efficiency (15th cycle) under BET, AnT and abiotic-control operations.

Fig 2: (a) UV-Vis Spectral profiles recorded at regular time intervals of different experimental variations and comparative spectrum of BET, AnT and Control operations. (b) Comparison of Substrate degradation rate and COD removal efficiency with respect to BET, AnT and abiotic-control operations

Fig 3: (a) Change in Azo reductase enzyme activity profiles of various experimental conditions studied with respect to regular time intervals. (b) Comparative evaluation of Dehydrogenase activity studied at regular time intervals.

Fig 4: (a) Bio-Electrogenic activity in terms of OCV and PD for BET and control operations. (b) Polarization Curve and anode potential measured at various resistances during stabilized performance for BET and abiotic-control operations.

Fig 5: (a) Electrochemical (Redox) behaviour of BET, AnT and abiotic-control operations recorded (scan rate; 30 mV/s) at regular time intervals and comparative evaluation of voltammograms recorded at 6 h under varying operating conditions (b) Timely varied first DCV profiles at varying operations of BET, AnT and control reactors.

Fig 6: Variation of Tafel plots along with redox Tafel slopes and polarization resistance variations with the function of BET, AnT and abiotic-control operations.

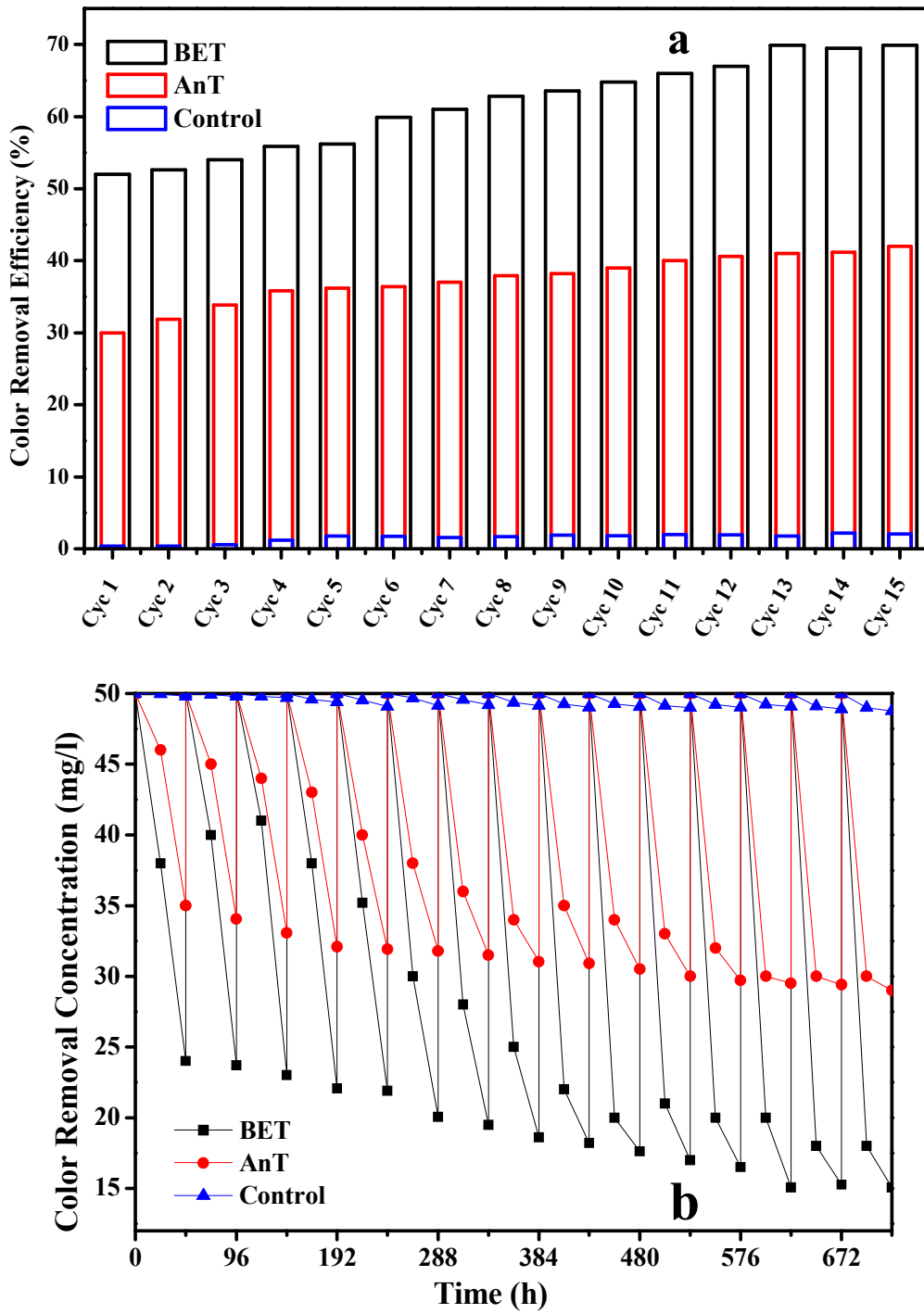


Fig 1

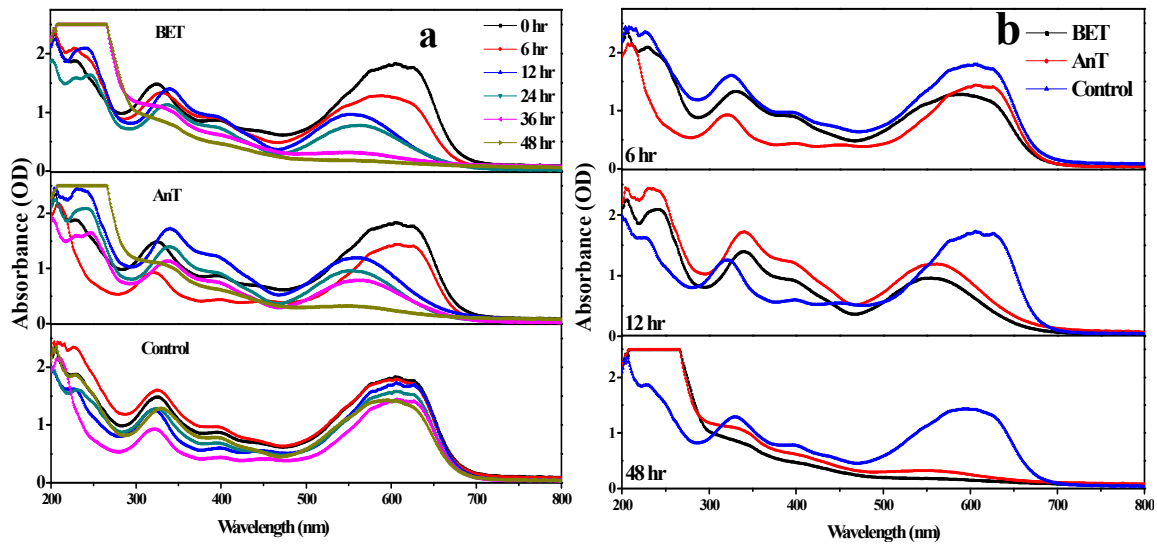


Fig 2a

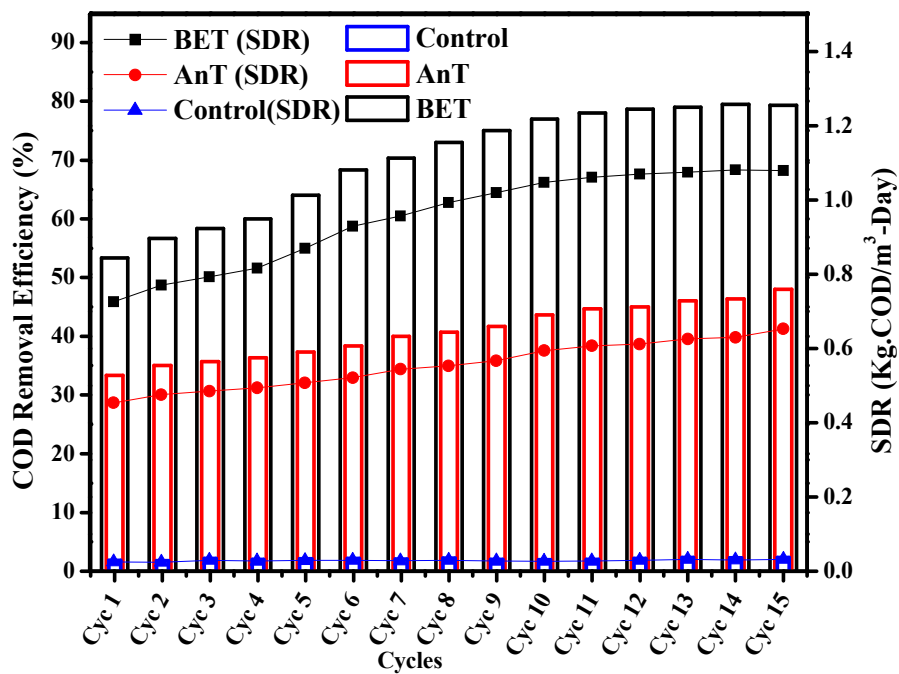


Fig 2b

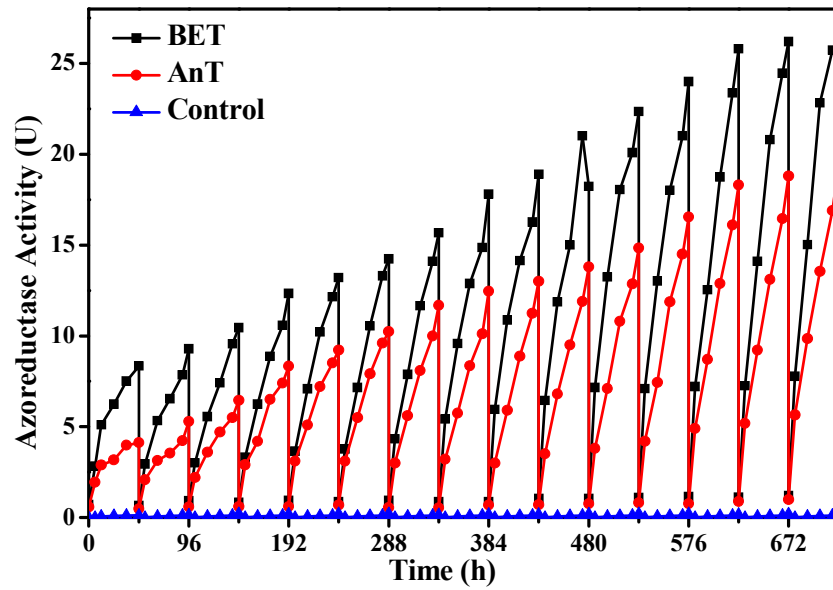


Fig 3a

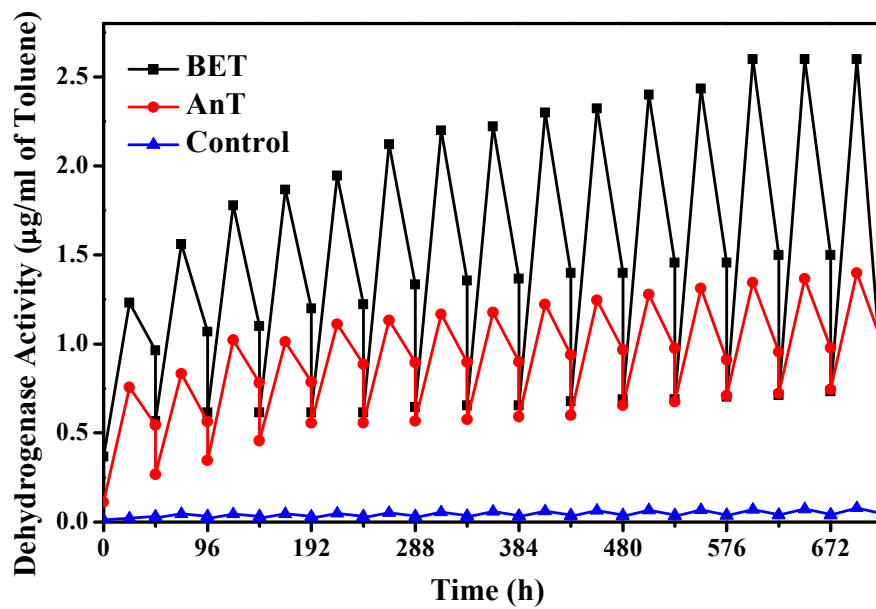


Fig 3b

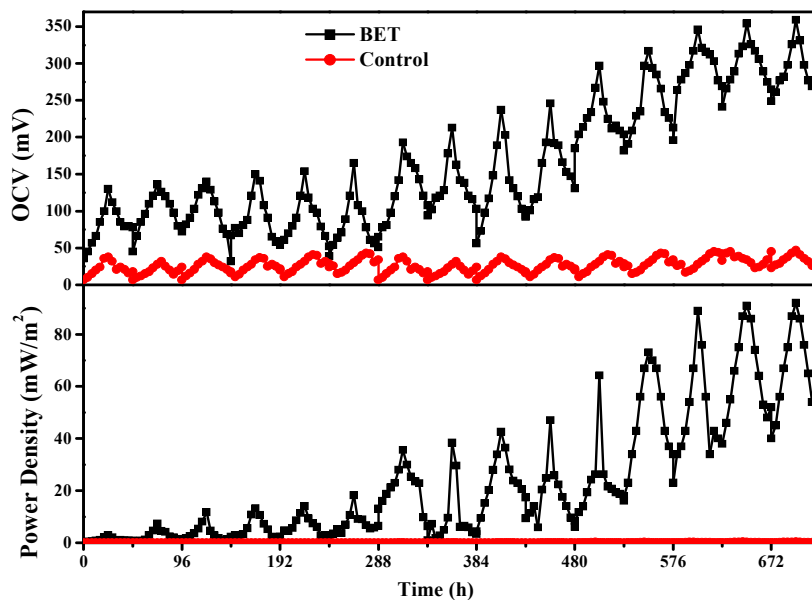


Fig 4a

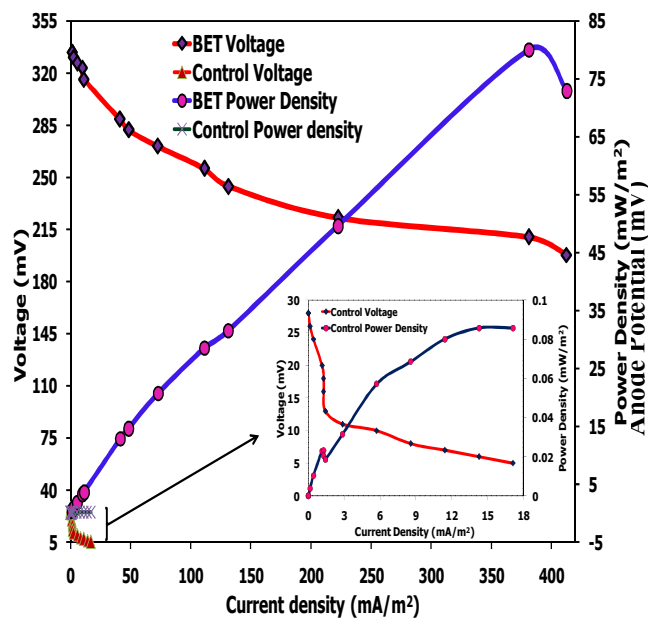


Fig 4b

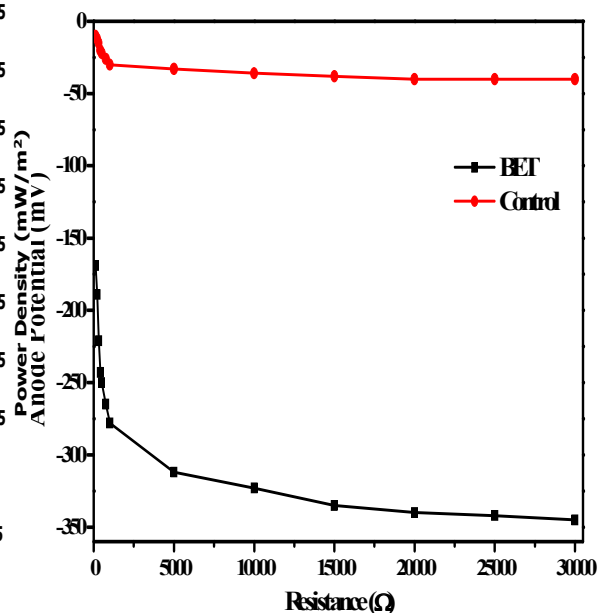


Fig 4c

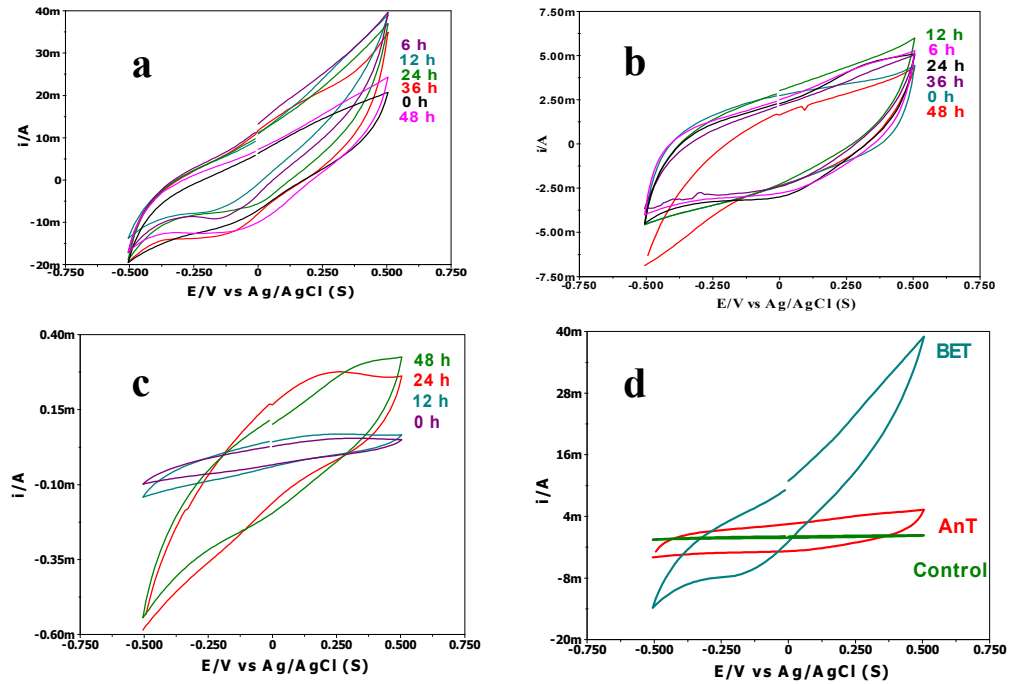


Fig 5a

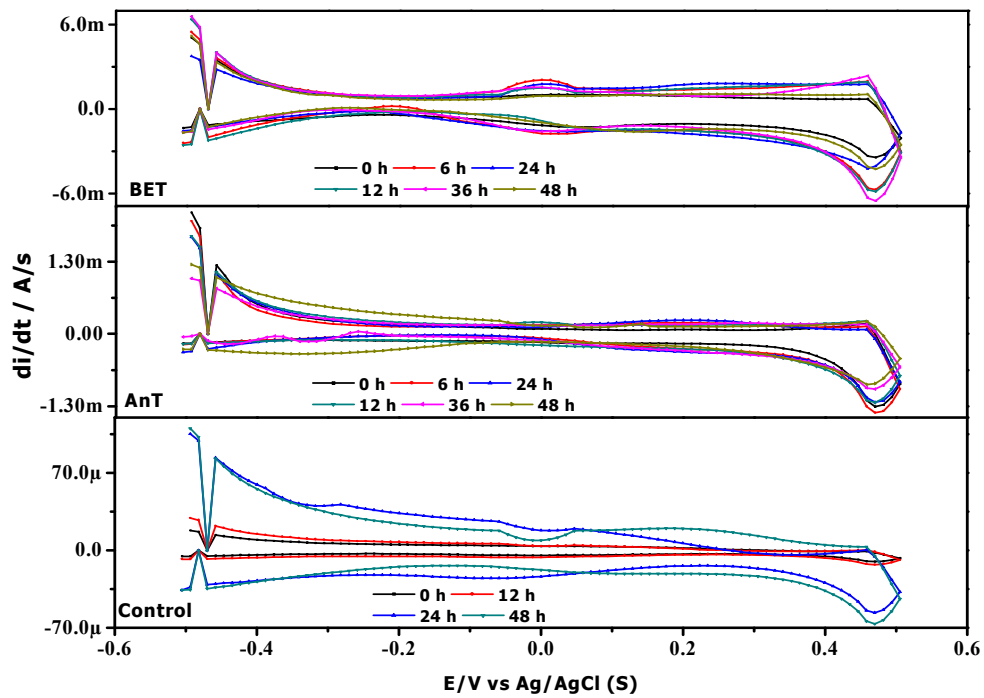


Fig 5b

